Supplementary Material

Impact of the 2Fe2P core geometry on the reduction chemistry of phosphido-bridged diiron hexacarbonyl compounds

Odi Th. E. Selan[A,B], *Mun Hon Cheah*[A,C,*], *Brendan F. Abrahams*[A], *Robert W. Gable*[A] and *Stephen P. Best*[A,*]

[A]School of Chemistry, The University of Melbourne, Parkville, Melbourne, 3010, Vic., Australia.

[B]Department of Chemistry, Faculty of Science and Engineering, Nusa Cendana University, Kupang – NTT, 85001, Indonesia.

[C]Department of Chemistry, Molecular Biometics, Ångström Laboratory, Uppsala University, SE 75237 Uppsala, Sweden.

*Correspondence to: Email: spbest@unimelb.edu.au, michael.cheah@kemi.uu.se

Impact of the 2Fe2P Core Geometry on the Reduction Chemistry of Phosphido-Bridged Diiron Hexacarbonyl Compounds

Odi Th. E. Selan,[1,2] Mun Hon Cheah,*[1,3] Brendan F. Abrahams[2], Robert W. Gable[2] and Stephen P. Best[2]*

The University of Melbourne, Melbourne, Victoria, 2010, Australia.

Supporting information

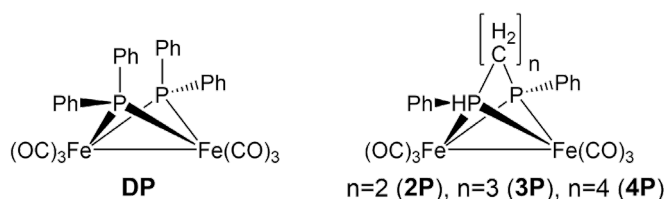**Nomenclature used to identify the phosphido-bridged diiron compounds**

Table S1: Crystal data and structure refinement of **2P**.

Table S2: Crystal data and structure refinement of **4P**.

Table S3: Selected bond lengths and bond angles of **2P** and **4P**.

Scheme S1: Double squares scheme as an alternate model of the electrochemistry of **2P**.

Figure S1: Cyclic voltammetry of **2P** in THF (0.1 M TBAPF$_6$) and simulation based on the double square scheme summarised in Scheme S1.

Table S4: Details of the parameters used to simulate the cyclic voltammetry of **2P** and **4P** shown in main text figures 2 and 3.

Figure S2: IR-SEC measurements during the reduction and reoxidation of **2P** in THF.

Figure S3: IR-SEC cell response during the experiment shown in Fig. S2.

Figure S4: Simulation of the CV of **2P** including concentration profiles calculated during reduction.

Figure S5: Simulation of the cyclic voltammetry of mixtures of the phosphido-bridged diiron hexacarbonyl compounds and ferrocene.

Table S5: Simulation parameters for ferrocene calibration of the phosphido-bridged diiron hexacarbonyl compounds.

Figure S6: Simulation of the cyclic voltammetry of 1°-phosphido bridged diiron hexacarbonyl compounds such as Fe$_2$(PH(CH$_2$Fc))$_2$(CO)$_6$. The compound and voltammetry is reported in reference [1] where the axial/equatorial isomers are labelled as **2a** and **2b**.

Figure S7: Structure of a DFT optimised dimer of [**2P2P**]$^{4-}$.

[1] School of Chemistry, The University of Melbourne, Parkville, Melbourne, 3010, Victoria, Australia
[2] Present address: Department of Chemistry, Faculty of Science and Engineering, Nusa Cendana University, Kupang - NTT, 85001, Indonesia
[3] Department of Chemistry, Molecular Biometics, Ångström Laboratory, Uppsala University, SE 75237 Uppsala, Sweden

Table S1: Crystal data and structure refinement of **2P**.

Identification code	SPB_02
Empirical formula	$C_{20}H_{14}Fe_2O_6P_2$
Formula weight	523.95
Temperature/K	130(2)
Crystal system	monoclinic
Space group	$P2_1/n$
a/Å	12.2037(8)
b/Å	11.7826(8)
c/Å	15.1800(10)
α/°	90
β/°	102.5500(10)
γ/°	90
Volume/Å³	2130.6(2)
Z	4
ρ_{calc}g/cm³	1.633
μ/mm⁻¹	1.546
F(000)	1056.0
Crystal size/mm³	0.2 × 0.2 × 0.1
Radiation	MoKα (λ = 0.71073)
2Θ range for data collection/°	3.894 to 56.562
Index ranges	-15 ≤ h ≤ 16, -15 ≤ k ≤ 11, -19 ≤ l ≤ 19
Reflections collected	13304
Independent reflections	5022 [R_{int} = 0.0241, R_{sigma} = 0.0311]
Data/restraints/parameters	5022/0/271
Goodness-of-fit on F^2	1.033
Final R indexes [I>=2σ (I)]	R_1 = 0.0282, wR_2 = 0.0695
Final R indexes [all data]	R_1 = 0.0331, wR_2 = 0.0720
Largest diff. peak/hole / e Å⁻³	0.46/-0.38

Table S2: Crystal data and structure refinement of **4P**.

Identification code	SPB_04
Empirical formula	$C_{22}H_{18}Fe_2O_6P_2$
Formula weight	552.01
Temperature/K	130(2)
Crystal system	monoclinic
Space group	$P2_1/n$
a/Å	16.09520(10)
b/Å	13.80620(10)
c/Å	20.8322(2)
α/°	90
β/°	100.6280(10)
γ/°	90
Volume/Å^3	4549.78(6)
Z	8
ρ_{calc}g/cm^3	1.612
μ/mm^{-1}	11.882
F(000)	2240
Crystal size/mm^3	0.39 × 0.35 × 0.20
Radiation	CuKα (λ = 1.54184)
2Θ range for data collection/°	3.200 to 67.133
Index ranges	-19 ≤ h ≤ 16, -16 ≤ k ≤ 16, -24 ≤ l ≤ 24
Reflections collected	29437
Independent reflections	8132 [R_{int} = 0.1242, R_{sigma} = 0.0939]
Data/restraints/parameters	8132/15/577
Goodness-of-fit on F^2	1.031
Final R indexes [I>=2σ (I)]	R_1 = 0.0556, wR$_2$ = 0.1412
Final R indexes [all data]	R_1 = 0.0630, wR$_2$ = 0.1489
Largest diff. peak/hole / e Å^{-3}	0.74/-1.39

Table S3: Selected bond lengths and bond angles of **2P** and **4P**.[†]

	4P$_a$	ESD*	**4P$_b$**	ESD	**2P**	ESD
Fe-Fe	2.6298	(8)	2.6333	(8)	2.6318	(4)
[Fe-P]$_{av}$	2.2153	0.0079	2.2191	0.0156	2.2037	0.0103
[Fe-C(O)]$_{av}$	1.7854	0.0155	1.7872	0.0117	1.7905	0.0117
[C-O]$_{av}$	1.1432	0.0096	1.1452	0.0087	1.1378	0.0032
[P-C$_{alkyl}$]$_{av}$	1.8490	0.0100	1.8440	0.0040	1.8431	0.0014
[P-C$_{aryl}$]$_{av}$	1.8285	0.0010	1.8290	0.0060	1.8091	0.0094
[C-C$_{alkyl}$]$_{av}$	1.5250	0.0069	1.5237	0.0071	1.5320	(3)
[C-C$_{aryl}A$]$_{av}$	1.3885	0.0088	1.3903	0.0066	1.3853	0.0063
[C-C$_{aryl}B$]$_{av}$	1.3867	0.0103	1.3897	0.0125	1.3862	0.0078
Angles						
P-Fe-Fe	53.7	0.2	53.7	0.5	53.3	0.4
P-Fe-P	80.6	0.2	81.6	0.1	72.4	0.1
Fe-P-Fe	72.8	0.3	72.8	0.1	73.3	0.1
Fe-C-O	177.6	0.5	177.1	0.7	177.7	1.0
Torsion						
P-Fe-Fe-P	107.0		108.6		94.8	
C$_{ap}$-Fe-Fe-C$_{ap}$	13.1		31.4		8.7	

[†] *The two crystallographically independent molecules of **4P** are labelled **4P$_a$** and **4P$_b$**.*

* *The error in a single value is given by the ESD from the X-ray analysis and the uncertainty in the last significant figure is given in parentheses, if the average is taken from two values then the ESD is given by the difference between the two values, in other cases the ESD is calculated.*

Scheme S1: Double squares scheme as an alternate model of the electrochemistry of **2P**.

2P

-1.59 V
0.005 cm s⁻¹

[2P]¹⁻ $K=3.9\times10^3$ [2P']¹⁻ $K=7.4\times10^{-12}$ [2P$_w$]¹⁻
         $k_f = 1$ $k_f = 1$

-1.70 V   -1.38 V   -0.68 V
0.005 cm s⁻¹   0.01 cm s⁻¹   0.005 cm s⁻¹

[2P]²⁻ $K=1\times10^3$ [2P']²⁻ $K=5$ [2P$_w$]²⁻
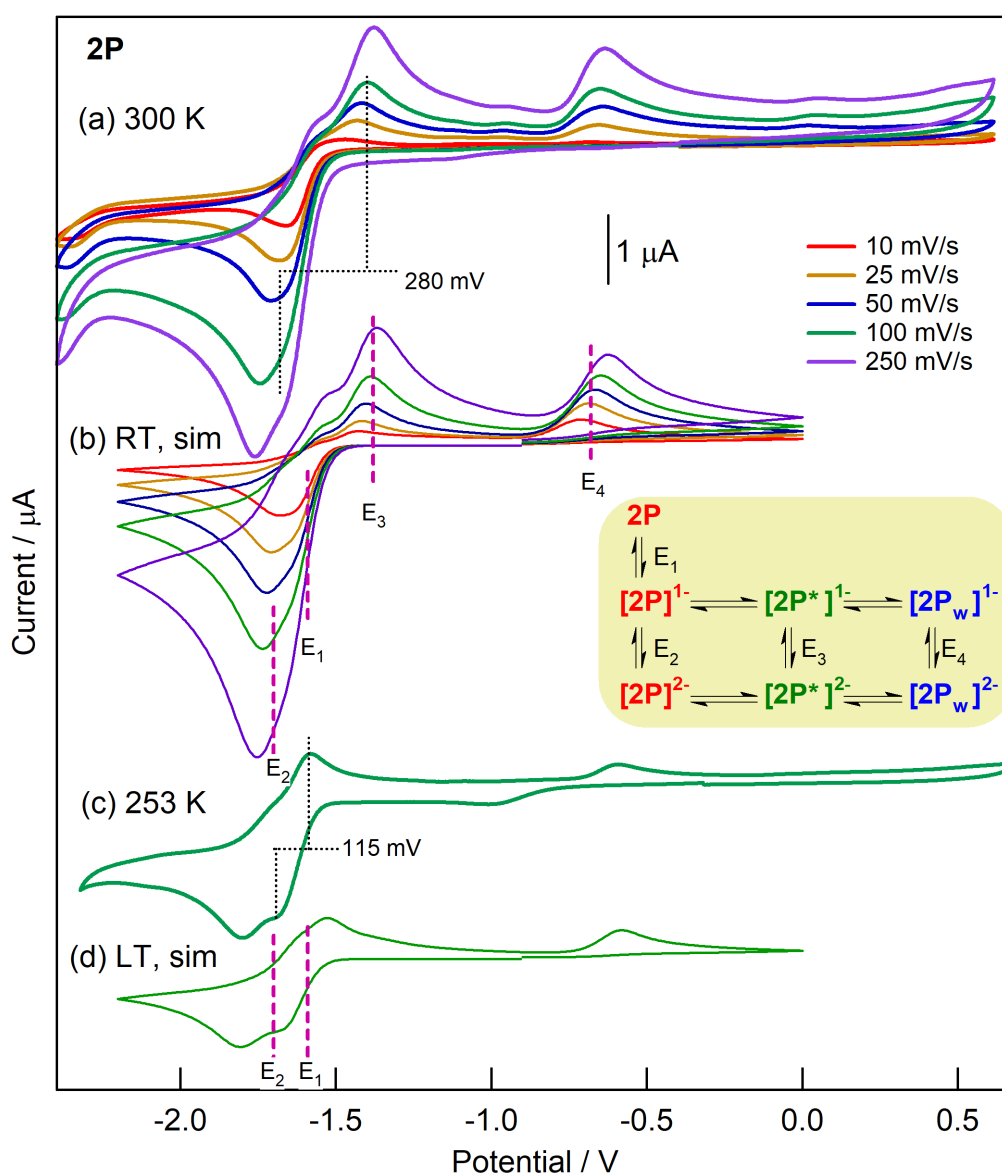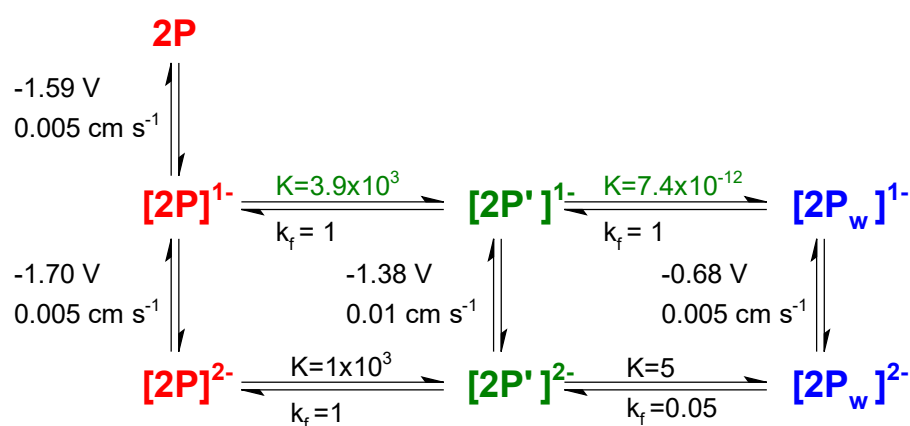 $k_f =1$ $k_f =0.05$

Figure S1: Observed and simulated cyclic voltammetry of **2P** in THF (0.1 M TBAPF₆). Potentials are given with respect the SHE. The simulation parameters are summarised in Scheme S1.

Table S4. *Details of the parameters used to simulate the cyclic voltammetry of **2P** and **4P** shown in main text figures 2 and 3.*

Species	Species {D/(cm^2/s), C$_{init}$ / M}		
2P {1×10^{-5}, 0.001}	**2Pm** {1×10^{-5}, 0}	**2Pwm** {1×10^{-5}, 0}	**2P2P3m** {1×10^{-5}, 0}
	2P2m {1×10^{-5}, 0}	**2Pw2m** {1×10^{-5}, 0}	**2P2P4m** {1×10^{-5}, 0}
Charge-transfer reactions	E°/V	RT, α, k_s(cm/s)	LT, α, k_s(cm/s)
2P + e = **2Pm**	-1.575	0.5, 0.01	0.5, 0.0075
2Pm + e = **2P2m**	-1.675	0.4, 0.005	0.4, 0.0025
2Pwm + e = **2Pw2m**	-0.655	0.4, 0.005	0.4, 0.0025
2P2P3m + e = **2P2P4m**	-1.375	0.5, 0.01	0.5, 0.0075
Chemical reactions	K_{eq}	RT, k_f, k_b	LT, k_f, k_b
2Pm + **2Pm** = **2P** + **2P2m**	0.020416	200, 9797	100, 9817
2Pm = **2Pwm**	5.8×10^{-15}	2×10^{-15}, 0.346	1×10^{-19}, 0.021
2P2m = **2Pw2m**	1000	2, 0.002	0.5, 0.0005
2Pm + **2Pw2m** = **2P2P3m**	1000	5×10^4, 50	100, 0.1
2P2m + **2Pw2m** = **2P2P4m**	1.18×10^8	0, 0	0, 0
Species	Species {D/(cm^2/s), C$_{init}$ / M}		
	4P {1×10^{-5}, 0.001}	**4Pm** {1×10^{-5}, 0}	**4P2m** {1×10^{-5}, 0}
Charge-transfer reactions	E°/V	RT, α, k_s(cm/s)	LT, α, k_s(cm/s)
4P + e = **4Pm**	-1.472	0.5, 0.015	0.5, 0.004
2Pm + e = **2P2m**	-1.262	0.6, 0.008	0.6, 0.0003
Chemical reactions	K_{eq}	RT, k_f, k_b	LT, k_f, k_b
4Pm + **4Pm** = **4P** + **4P2m**	3541	1000, 0.28	500, 0.033

Values printed in red are fixed by thermodynamic relationships. Simulations were conducted using DigiElch[2] – Professional build 8.225 with a planar electrode geometry (area = 0.007 cm^2), the uncompensated resistance and capacitance were set to zero and diffusion was treated using a semi-infinite 1D model. For RT simulations the temperature was set to 298 K, LT simulations were calculated for a temperature of 253 K.

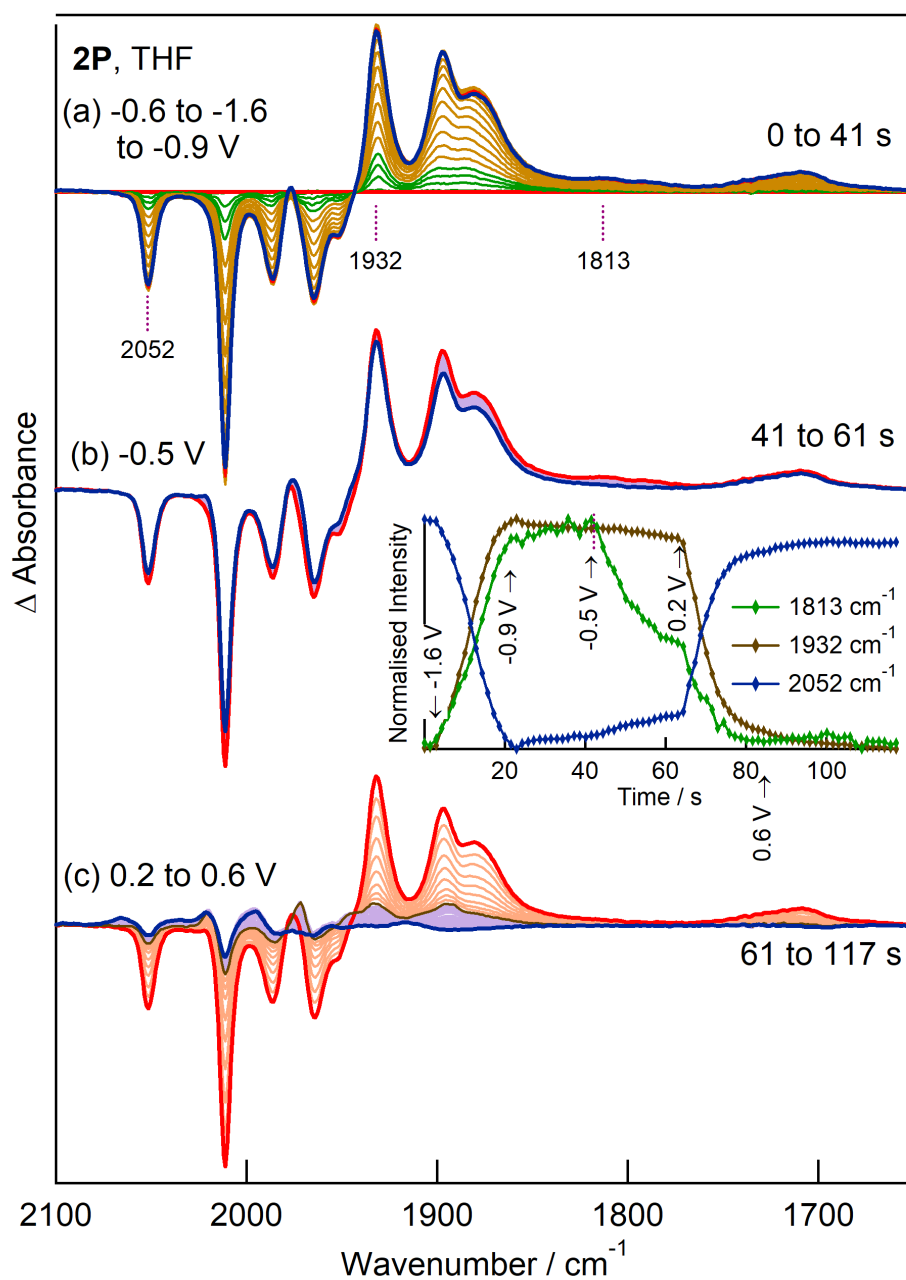IR-SEC measurements during the reduction and reoxidation of **2P** in THF.

Figure S2: IR-SEC measurements during reduction and reoxidation of a 1 mM solution of **2P** in THF (0.2 M TBAPF₆). Potentials are given with respect to a Ag disc pseudo-reference electrode and are offset by ca. 0.3 V w.r.t. the NHE. The current response to the changes in potential are given in the following figure (Fig. S2).
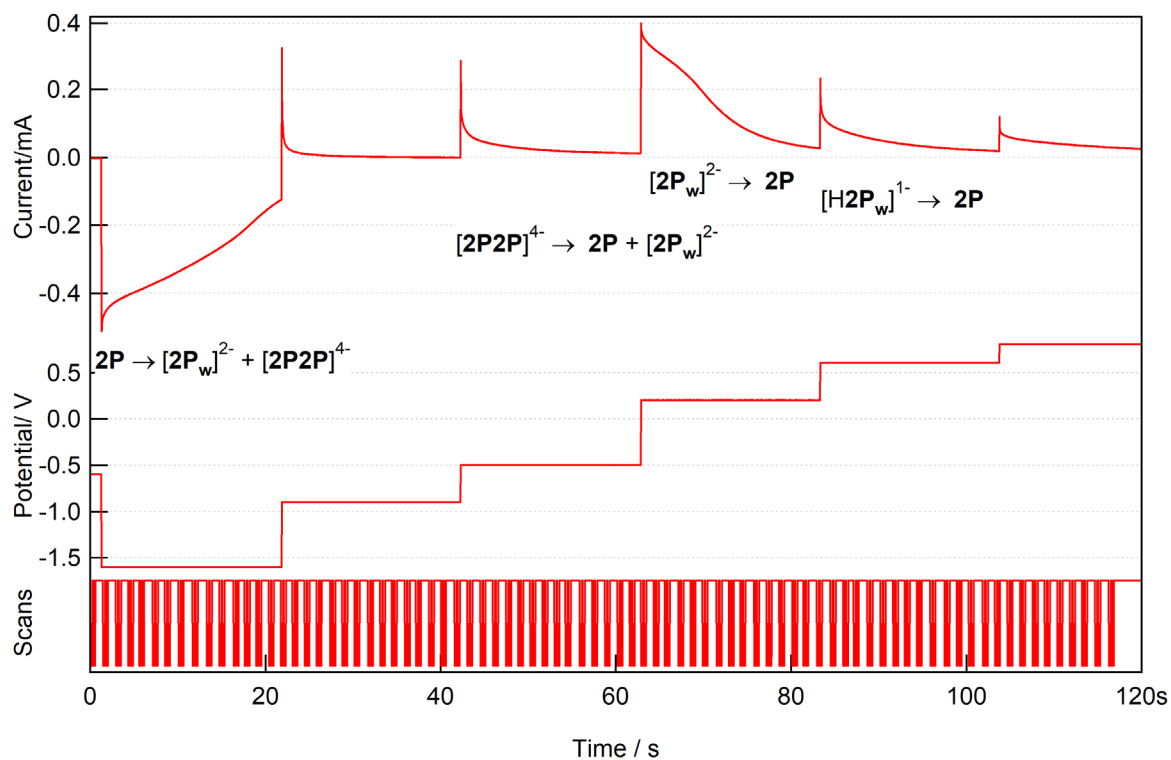
Figure S3: IR-SEC cell response during the experiment shown in Fig. S2. The scans trace corresponds to the TTL signal from the FTIR spectrometer which reports the zero path difference state of the interferometer and this corresponds to the start of the IR scan. Each spectrum comprises two scans.
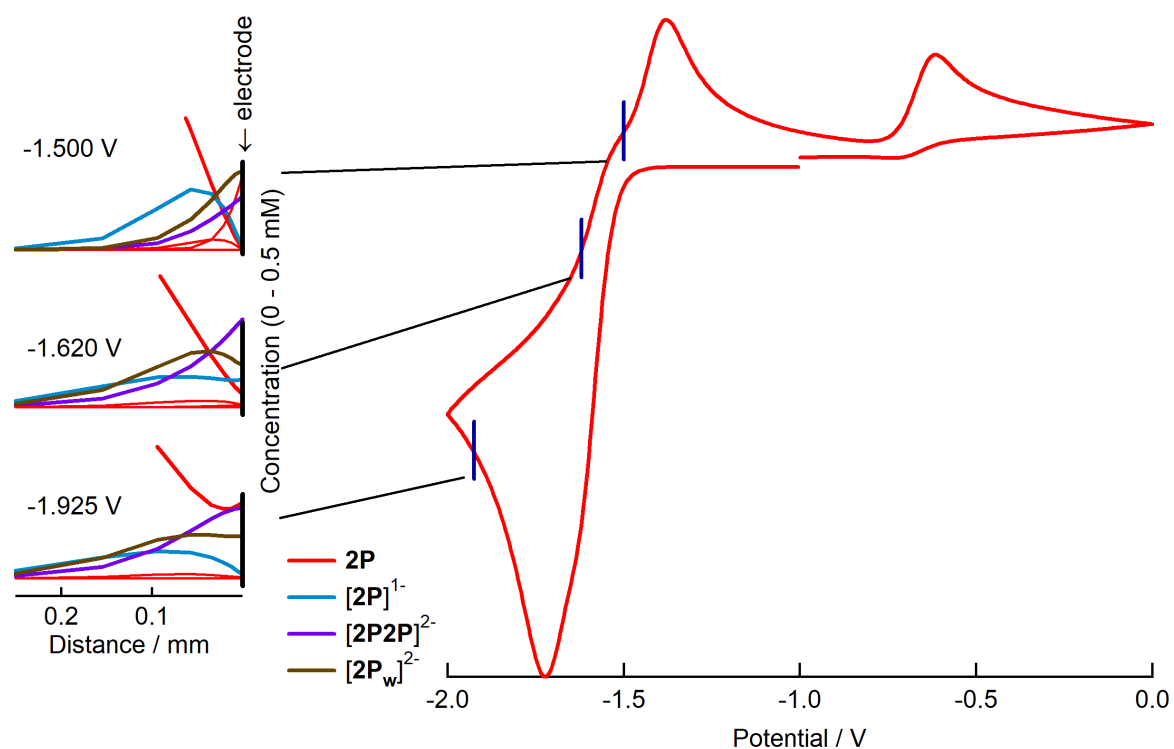
Figure S4: *Simulation of the CV of **2P** including concentration profiles calculated during reduction. The relative concentrations of [**2P2P**]$^{2-}$ and [**2P$_w$**]$^{2-}$ which when integrated over a thin film (20 μm) change during the reduction stage of the reaction. The relative concentration of [**2P2P**]$^{2-}$ is lower than that of [**2P$_w$**]$^{2-}$ for measurements conducted in THF relative to more coordinating solvents such as CH$_3$CN.*

DP + Fc, THF

$E_1 = -1.362$ V
$E_2 = -1.152$ V

10 µA

4P + Fc, THF

$E_1 = -1.472$ V
$E_2 = -1.262$ V

1 µA

3P + Fc, THF

$E_1 = -1.554$ V
$E_2 = -1.532$ V

1 µA

2P + Fc, THF

$E_1 = -1.575$ V
$E_2 = -1.675$ V
$E_3 = -0.655$ V
$E_4 = -1.375$ V
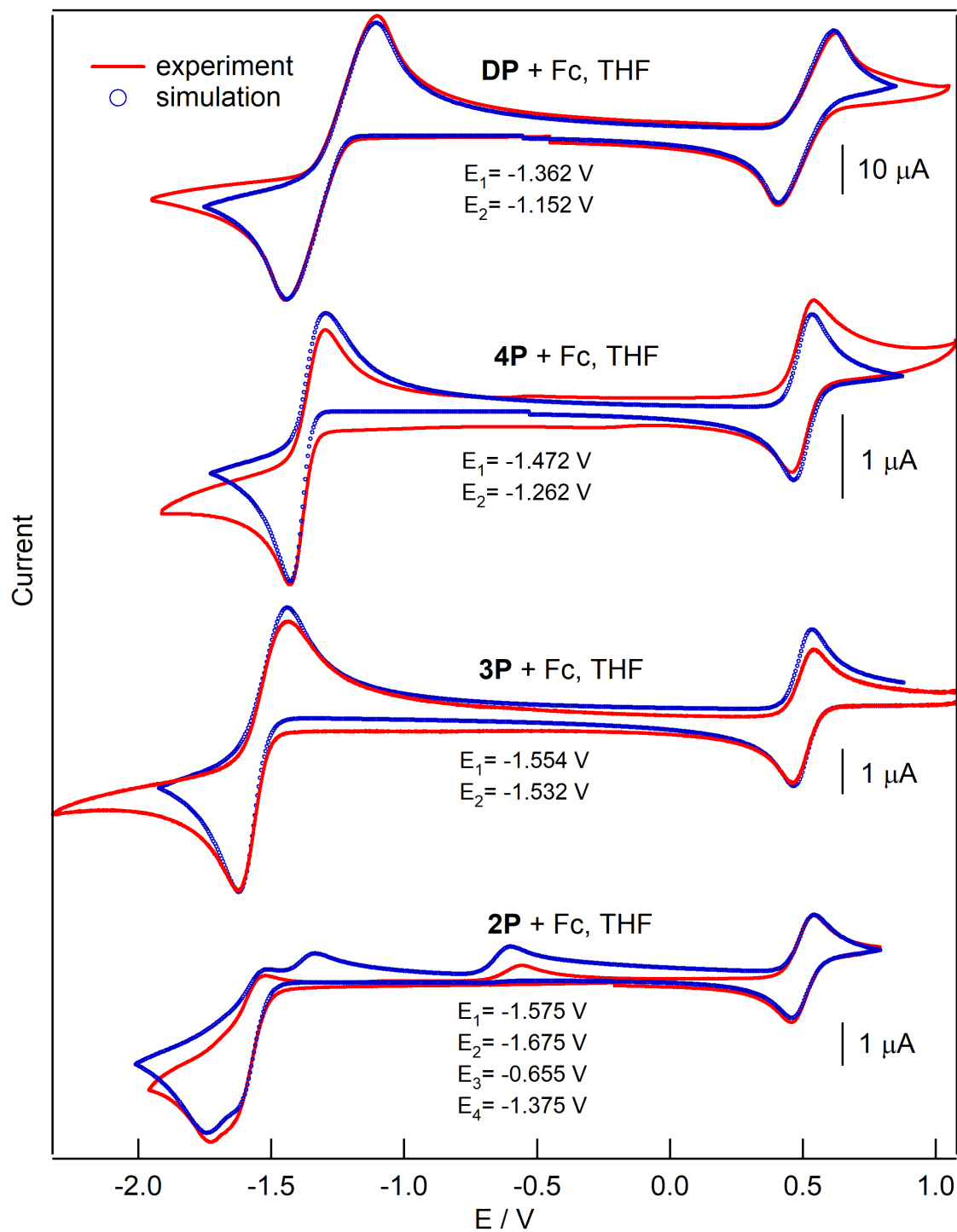
1 µA

— experiment
○ simulation

Current

E / V

Figure S5: Simulation of the cyclic voltammetry of mixtures of the phosphido-bridged diiron hexacarbonyl compounds and ferrocene.

Table S5: Simulation parameters for ferrocene calibration of the phosphido-bridged diiron hexacarbonyl compounds.

Species	Species {D/(cm^2/s), C_{init} / M}		
2P {1×10^{-5}, 0.0015}, **2Pm, 2P2m, 2Pwm, 2Pw2m, 2P2P3m, 2P2P4m** {1×10^{-5}, 0}			
Fc {1×10^{-5}, 0.0008}, **Fcp** {1×10^{-5}, 0}			
Charge-transfer reactions	$E°/V$	RT, α, $k_s(cm/s)$	
2P + e = **2Pm**	-1.575	0.5, 0.01	
2Pm + e = **2P2m**	-1.675	0.4, 0.005	
2Pwm + e = **2Pw2m**	-0.655	0.4, 0.005	
2P2P3m + e = **2P2P4m**	-1.375	0.5, 0.01	
Fcp + e = **Fc**	+0.5	0.5, 0.01	
Chemical reactions	K_{eq}	RT, k_f, k_b	
2Pm + **2Pm** = **2P** + **2P2m**	0.020416	1000, 5×10^4	
2Pm = **2Pwm**	5.8×10^{-15}	2×10^{-15}, 0.346	
2P2m = **2Pw2m**	1000	2, 0.002	
2Pm + **2Pw2m** = **2P2P3m**	1000	1000, 1	
2P2m + **2Pw2m** = **2P2P4m**	1.18×10^8	0, 0	
Species	Species {D/(cm^2/s), C_{init} / M}		
3P {1×10^{-5}, 0.0012}, **Fc** {{1×10^{-5}, 0.001}, **3Pm** ,**3P2m, Fcp** {1×10^{-5}, 0}			
Charge-transfer reactions	$E°/V$	RT, α, $k_s(cm/s)$	
3P + e = **3Pm**	-1.554	0.7, 0.005	
3Pm + e = **3P2m**	-1.532	0.6, 0.001	
Fcp + e = **Fc**	+0.5	0.5, 0.025	
Chemical reactions	K_{eq}	RT, k_f, k_b	
3Pm + **3Pm** = **3P** + **3P2m**	2.35	1000, 4248	

Species	Species {D/(cm²/s), C_init / M}		
4P {1×10⁻⁵, 0.00055}, **Fc** {{1×10⁻⁵, 0.00062}, **4Pm**, **4P2m**, **Fcp** {1×10⁻⁵, 0}			

Charge-transfer reactions	$E°/V$	RT, α, $k_s(cm/s)$	
4P + e = **4Pm**	-1.472	0.5, 0.025	
4Pm + e = **4P2m**	-1.262	0.6, 0.01	
Fcp + e = **Fc**	+0.5	0.5, 0.025	
Chemical reactions	K_{eq}	RT, k_f, k_b	
4Pm + **4Pm** = **4P** + **4P2m**	3540	10000, 2.8	

Species	Species {D/(cm²/s), C_init / M}		
DP {1×10⁻⁵, 0.0115}, **Fc** {{1×10⁻⁵, 0.013}, **DPm**, **DP2m**, **Fcp** {1×10⁻⁵, 0}			

Charge-transfer reactions	$E°/V$	RT, α, $k_s(cm/s)$	
DP + e = **DPm**	-1.362	0.5, 0.02	
DPm + e = **DP2m**	-1.152	0.5, 0.015	
Fcp + e = **Fc**	+0.5	0.5, 0.02	
Chemical reactions	K_{eq}	RT, k_f, k_b	
DPm + **DPm** = **DP** + **DP2m**	3541	10000, 2.8	

Ru = 0 (**2P**, **3P**, **4P**) or 3000 Ohm (**DP**), WE area = 0.007 cm², Semi-infinite 1D diffusion

Chemical Reactions

$[Fe_2(PH)_2]^{1-} + [Fe_2(PH)_2]^{1-} = Fe_2(PH)_2 + [Fe_2(PH)_2]^{2-}$ $K = 343^*$ k_f 1×10^4 1×10^4

$[Fe_2(PH)_2]^{1-} + [Fe_2(PH)_2]^{1-} = 2[Fe_2(P)(PH)]^{1-} + H_2$ $K = 3 \times 10^6$ k_f 0 1×10^4

$Fe_2(PH)_2 + [Fe_2(PH)_2]^{2-} = 2[Fe_2(P)(PH)]^{1-} + H_2$ $K = 1 \times 10^4$ k_f 0 1×10^5

* fixed by thermodynamic relations

Common parameters
Area = 0.007 cm^2, ν = 0.1 V/s
Ru = 0 Ohm, Cdl = 0 F, 298 K
$E_1([\ ]^{0/1-})$ -2.05 V, n= 1, α = 0.5, k_s= 0.01 cm/s
$E_2([\ ]^{1-/2-})$ -1.90 V, n= 1, α = 0.5, k_s= 0.005 cm/s
$E_3([\ ]^{2+/0})$ 0 V, n= 2, α = 0.5, k_s= 0.01 cm/s
$Fe_2(PH)_2$ = 1 mM, D = 1×10^{-5} all species

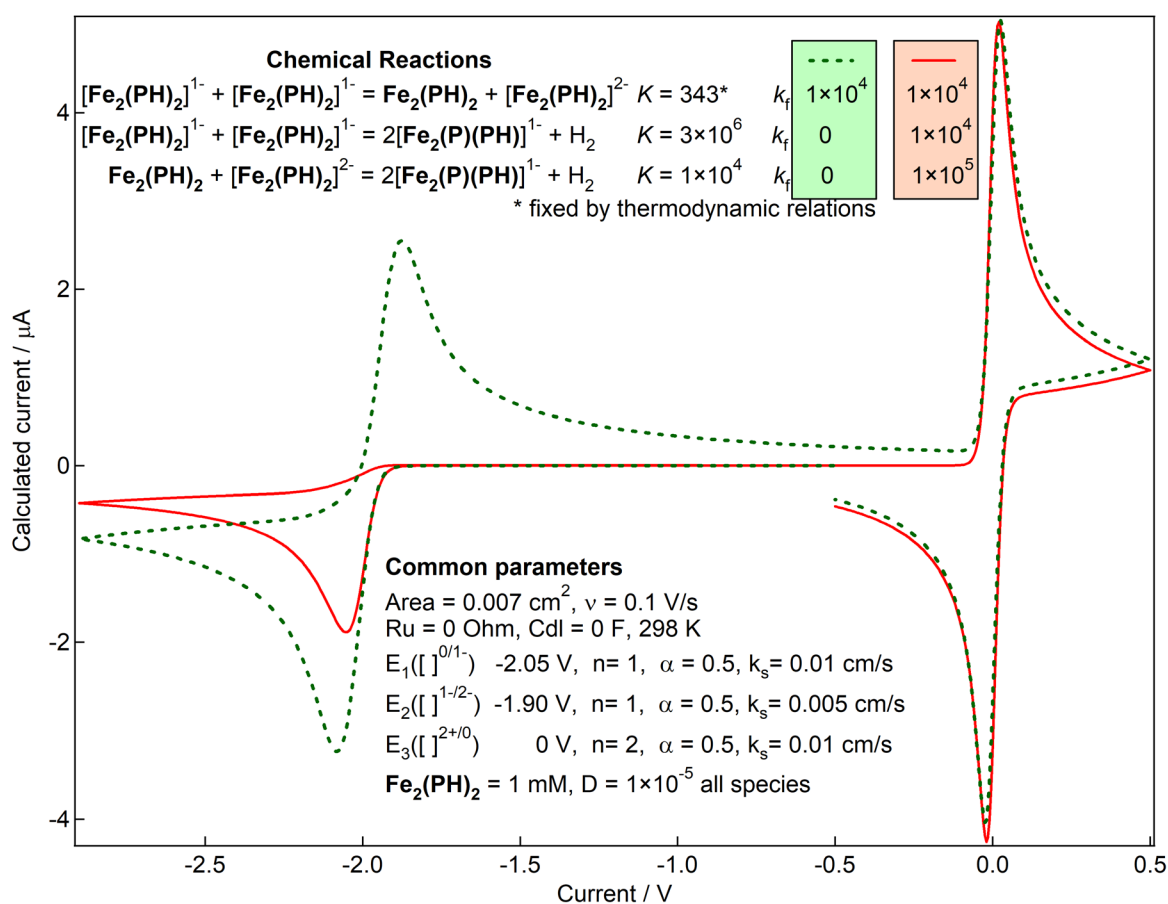*Figure S6: Simulation of the cyclic voltammetry of 1°-phosphido bridged diiron hexacarbonyl compounds such as Fe₂(PH(CH₂Fc))₂(CO)₆. The compound and voltammetry is presented in reference [1] where the axial/equatorial isomers are labelled as **2a** and **2b**. The electrochemistry was interpreted in that report in terms of there being only one reduction process for the parent diiron compound. The absence of a second reduction of the parent compound is not consistent with the accessibility of a planar 2Fe2P core for the 2-electron reduced species. The simulations shown include the second reduction process and have E₁ < E₂ (i.e. the monoanion is unstable with respect to disproportionation) in line with the observed electrochemistry for unlinked phosphido-bridged complexes. The dashed green line gives the simulation for the case where there is no following chemistry and the solid red line includes bimolecular reactions leading to dihydrogen formation with generation of the phosphinidene bridge. The simulation shows that the loss of the return wave near -2 V can follow 2-electron reduction with E₁ < E₃ as is normally observed for bis(phosphido) bridging ligands and provides a mechanistic path for elimination of dihydrogen. While the presence of a bulky ligand was shown to lower the rate of the reoxidation reaction,[1, 3] modification of the simulation to take into account such an effect would increase the parameter space for which there is no significant reoxidation wave for E₁, E₂ (as observed experimentally).*
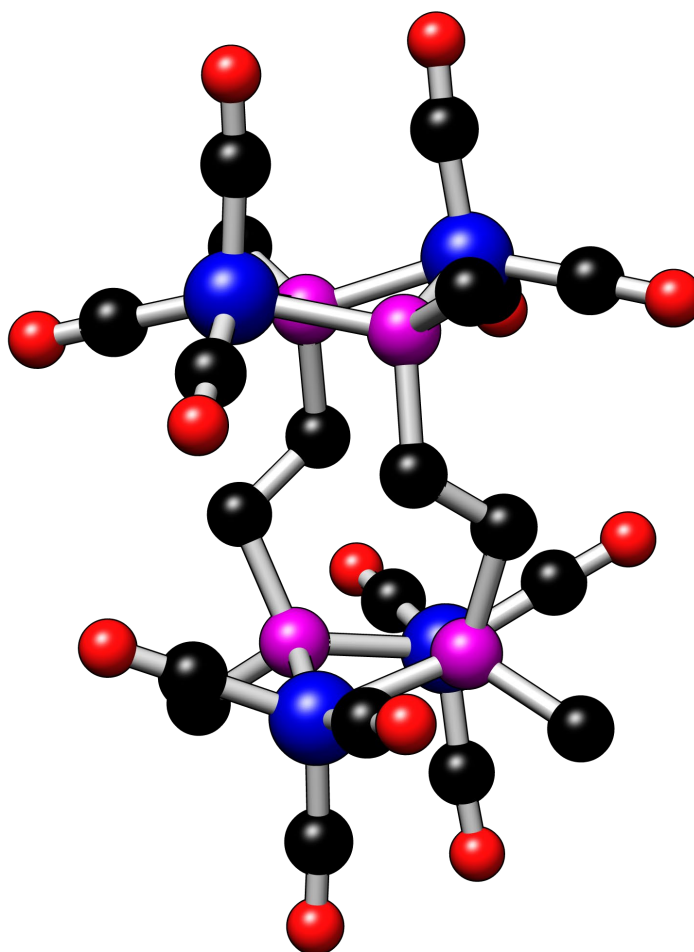
Figure S7*: Structure of a DFT optimised dimer of [**2P2P**]$^{4-}$. Fe atoms are coloured in blue, P atoms in cyan, C atoms in black and O atoms in red. Hydrogen atoms are removed for clarity. Phenyl groups are replaced with methyl groups to reduce computation time.*

References

1.   Gimbert-Surinach, C.; Bhadbhade, M.; Colbran, S. B., Bridgehead Hydrogen Atoms Are Important: Unusual Electrochemistry and Proton Reduction at Iron Dimers with Ferrocenyl-Substituted Phosphido Bridges. *Organometallics* **2012,** *31* (9), 3480-3491.

2.   Rudolph, M.; Reddy, D. P.; Feldberg, S. W., A Simulator for Cyclic Voltammetric Responses. *Anal. Chem.* **1994,** *66*, 589A-600A.

3.   Rahaman, A.; Gimbert-Surinach, C.; Ficks, A.; Ball, G. E.; Bhadbhade, M.; Haukka, M.; Higham, L.; Nordlander, E.; Colbran, S. B., Bridgehead isomer effects in *bis*(phosphido)-bridged diiron hexacarbonyl proton reduction electrocatalysts. *Dalton Trans.* **2017,** *46* (10), 3207-3222.